A computational study of hydration, solution structure, and dynamics in dilute carbohydrate solutions

Sau Lawrence Lee and Pablo G. Debenedetti[a)]
Department of Chemical Engineering, Princeton University, Princeton, New Jersey 08544

Jeffrey R. Errington
Department of Chemical Engineering University at Buffalo, The State University of New York, Buffalo, New York 14260-4200

(Received 26 January 2005; accepted 25 March 2005; published online 27 May 2005)

We report results from a molecular simulation study of the structure and dynamics of water near single carbohydrate molecules (glucose, trehalose, and sucrose) at 0 and 30 °C. The presence of a carbohydrate molecule has a number of significant effects on the microscopic water structure and dynamics. All three carbohydrates disrupt the tetrahedral arrangement of proximal water molecules and restrict their translational and rotational mobility. These destructuring effects and slow dynamics are the result of steric constraints imposed by the carbohydrate molecule and of the ability of a carbohydrate to form stable H bonds with water, respectively. The carbohydrates induce a pronounced decoupling between translational and rotational motions of proximal water molecules. © *2005 American Institute of Physics*. [DOI: 10.1063/1.1917745]

I. INTRODUCTION

Carbohydrates have been shown to be effective stabilizers of biological components, such as proteins and membranes, in the aqueous, frozen, and dehydrated states.[1–5] The addition of carbohydrates, such as trehalose and sucrose, to liquid and solid pharmaceutical formulations effectively improves their shelf life by maintaining the structural and functional integrity of labile biomolecules in the formulations.[6,7] The detailed modes by which particular carbohydrates stabilize and protect biological molecules remain incompletely understood. A number of interpretations have been proposed to explain their effectiveness as protein stabilizers under different conditions. It is generally accepted that preferential solute exclusion from the protein surface is responsible for the stabilizing effects of carbohydrates in an aqueous solution.[8] According to this mechanism, carbohydrate molecules are preferentially excluded from the protein's surface, increasing the protein's chemical potential. The degree of preferential exclusion and the chemical potential of the protein increase with the amount of protein surface area exposed to the solvent. Since proteins in the denatured state have a larger surface area than in the native state, this results in a correspondingly higher increase in chemical potential that stabilizes the more compact folded state. Thus, the native protein is preferentially hydrated and stabilized in an aqueous solution. This thermodynamic mechanism has also been invoked to explain protein stabilization by carbohydrates during freeze-thaw processes.[9,10]

Two mechanisms have been proposed to explain protein stabilization by carbohydrates during dehydration. The first one suggests that the carbohydrates improve protein stability because of their ability to form amorphous solids at low water contents.[11] In the glassy state, characterized by an extremely sluggish molecular motion, proteins are effectively immobilized and isolated from potentially reactive species, such as oxygen. Thus, reactions that reduce the biological activity of proteins, such as oxidation and disulfide rearrangement, are slowed down dramatically. According to a second viewpoint, carbohydrates protect the protein against drying stresses by serving as substitutes for water in the hydrogen-bond network during dehydration.[12] By maintaining the hydrophobic driving force towards folding throughout the drying process, the formation of hydrogen bonds between carbohydrates and proteins would, in this interpretation, help to preserve protein secondary and tertiary structure, and therefore enhance the activity recovery of the protein upon reconstitution.

Although knowledge of the detailed manner in which carbohydrates stabilize proteins remains incomplete, it is clear that water plays an important role in determining the physical and chemical stability of proteins in liquid and solid formulations. In both liquid and amorphous states, water serves as a solvent medium through which species must diffuse in order to react with proteins. Water can also increase the chemical reactivity of formulations by participating in reactions such as hydrolysis.[13] Water is a strong plasticizer[14,15] that depresses the glass transition temperature (T_g) of amorphous solids. The addition of water to the glassy carbohydrate matrix causes an increase in free volume and a decrease in viscosity. The resulting enhancement in molecular mobility has significant effects on the rates of diffusion and degradation processes,[16] such as aggregation.

Because of the importance of water in the chemical and physical degradation processes in formulations containing, primarily, proteins, carbohydrates, and water, a considerable amount of experimental work has been done to study water dynamics and structure in carbohydrate-water systems as a

[a)]Author to whom correspondence should be addressed. Electronic mail: pdebene@princeton.edu

function of carbohydrate concentration and temperature.[17–28] One of the interesting observations from these previous studies is the dynamical decoupling between water and carbohydrates. The NMR work of Girlich and Lüdemann showed that the rotational dynamics of water, described by a Vogel–Tammann–Fulcher (VTF) equation, becomes almost concentration independent at sucrose concentrations greater than 60 wt %. In this range of sugar concentrations, the ideal glass transition temperatures in the VTF equation, T_0, for water are almost constant and similar to that of neat water.[17,25] This is approximately in the range of carbohydrate concentrations over which Rampp *et al.* found a dramatic increase in the ratio of water to carbohydrate translational diffusivity with falling temperature using ^{13}C and proton NMR.[19] In addition, Champion *et al.* showed a decoupling between translational diffusion and viscosity in concentrated sucrose solutions near the glass transition temperature T_g using the fluorescence recovery after the photobleaching method.[24] There are neutron-scattering studies focusing on the microscopic mechanism of water diffusion in carbohydrate solutions. Magazù *et al.* reported a continuous diffusion and jump-diffusion mechanism for sugar and water, respectively, in a 46-wt % trehalose solution at 309 K.[27] Feeney *et al.* used the same technique to study water dynamics of 4, 29, and 60-wt % fructose solution at 300 K and found a transition from continuous to jump diffusion at 29-wt % fructose concentration.[26]

In the structural studies of carbohydrate-water mixtures, Branca *et al.* used the Raman scattering to investigate the effect of disaccharides (trehalose, maltose, and sucrose) on the hydrogen-bond network of water.[21] They showed that trehalose has a greater destructuring effect on the tetrahedral H-bond network of water in comparison to sucrose and maltose. They also emphasized that the superior effectiveness of trehalose in protecting biological components is related to its greater destructuring effect. Later, Branca *et al.* also performed density, viscosity, sound velocity, and inelastic neutron scattering measurements to further characterize the interactions between disaccharides and water.[28,29] Consistent with their previous argument, they stressed that the greater bioprotective ability of trehalose can be attributed to its stronger interactions with water (e.g., hydration number).

In addition to the above-mentioned experimental studies, several molecular dynamics simulations have been carried out to investigate the dynamics and structure of water in carbohydrate solutions.[30–43] The detailed hydration pattern around individual carbohydrate atoms was obtained by evaluating one- and two-dimensional radial distribution functions[31,35,40,41] and by calculating three-dimensional water density contours around the solute.[30,42,43] The important observation from these calculations is that carbohydrates, such as trehalose and sucrose, are well hydrated because of the ability of their hydroxyl groups to form H bonds with the surrounding water, as indicated by the first peak in the radial distribution of water around the carbohydrate hydroxyl groups. However, the effects of carbohydrates on the structural order of proximal water molecules, such as the extent to which a given water molecule and its surrounding neighbors adopt tetrahedral arrangements, have not been investigated systematically in previous computational works. Some simulation studies have investigated water dynamics in the vicinity of carbohydrates.[33,44,45] These reports showed a comparably lower translational mobility of hydration water around the carbohydrate. However, the origin of this slow dynamics and its possible relation to the H-bond network remain incompletely understood. In addition, the influence of carbohydrates on the rotational dynamics of vicinal water molecules has not been investigated extensively.

As a step towards answering some of these questions, the present work investigates the local structure and dynamics of hydration water in dilute carbohydrate solutions at 0 and 30 °C. We are particularly interested in comparing water structure and mobility near carbohydrates to the corresponding bulk properties. In the study of water structure, the orientational order parameter q,[46,47] which measures the tendency of a water molecule and its four nearest neighbors to adopt a tetrahedral arrangement, was used to quantify local and bulk water structures. In the study of water dynamics, the translational diffusion coefficient and rotational relaxation time of water were calculated as a function of distance from specific carbohydrate atoms. Water-water and water-carbohydrate H-bond dynamics were also analyzed and related to the slow dynamics of hydration water. Two disaccharides (trehalose and sucrose) and one monosaccharide (glucose) were selected for the present molecular dynamics investigation. Trehalose and sucrose have the same chemical formula ($C_{12}O_{11}H_{22}$) but differ in structure: trehalose contains two glucose rings, whereas sucrose contains one fructose and one glucose ring. Schematic representations of these three carbohydrates are shown in Fig. 1.

The remainder of this paper is organized as follows: Section II describes the molecular models and simulation methods used in this work. Results are presented in Section III. Section IV summarizes the main findings and suggests possible directions for further simulation studies of carbohydrate-water systems.

II. MOLECULAR MODEL AND SIMULATION METHODS

In this study, a modified Toukan and Rahman version (mTR)[48,49] of a SPC-type[50] water was used. This mTR model treats water as a fully flexible molecule, having a single Lennard-Jones (LJ) site centered on the oxygen atom and three partial atomic charges. One positive charge (+0.41 e) is placed on each of the two hydrogen atoms, and one negative charge (−0.82 e) is placed on the oxygen atom. The OH stretching and HOH bending are described by anharmonic intramolecular potentials. A detailed description of these intramolecular potentials is given elsewhere.[48] Similar to water, the carbohydrates (glucose, trehalose, and sucrose) were also modeled as fully flexible molecules using the Optimized Potential(s) for Liquid Simulation (OPLS) all-atom force field. Specifically, we used the parameter set optimized for carbohydrates.[51] The bonded interactions include stretching, bending, and torsion interactions. Bond stretching and bending were described by harmonic potentials given in

$$V_{\text{stretch}} = K_r(r - r_{\text{eq}})^2, \tag{1}$$

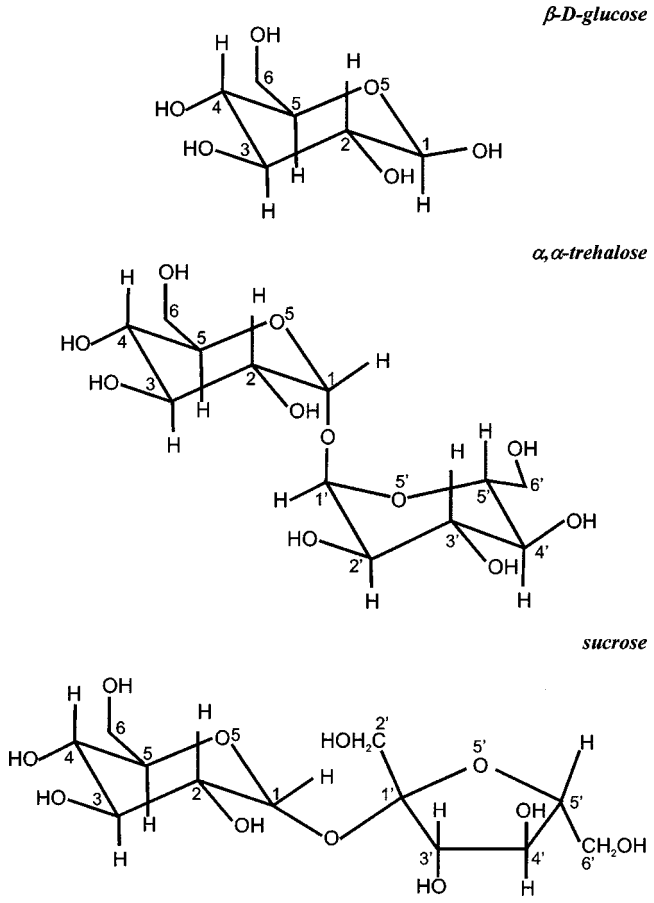

FIG. 1. Stick representation of the different geometries of the carbohydrates used in this work, indicating the numbering convention of carbon atoms (C). The oxygen that is covalently bonded to the carbon follows the same number convention. For example, O2 is the oxygen covalently bonded to C3. For trehalose and sucrose, O1 is the glycosidic oxygen.

$$V_{\text{bend}} = K_\theta(\theta - \theta_{\text{eq}})^2, \tag{2}$$

where K_r, K_θ, r_{eq}, and θ_{eq} are the stretching modulus, bending modulus, equilibrium bond length, and equilibrium bond angle, respectively. The torsional potential is described in

$$V_{\text{tor}} = \frac{V_1}{2}[1 + \cos(\phi)] + \frac{V_2}{2}[1 - \cos(2\phi)] + \frac{V_3}{2}[1 + \cos(3\phi)], \tag{3}$$

where ϕ is the dihedral angle, and V_1, V_2, and V_3 are the torsional parameters. The nonbonded interactions include Coulombic and Lennard-Jones interactions between atoms separated by three or more bonds as well as between sites on different molecules,

$$V_{nb} = \frac{q_i q_j}{4\pi\varepsilon_0 r} + 4\varepsilon_{ij}\left[\left(\frac{\sigma_{ij}}{r}\right)^{12} - \left(\frac{\sigma_{ij}}{r}\right)^{6}\right], \tag{4}$$

where r is the separation distance between atoms i and j, q_i is the value of the partial charge on atom i, and ε_{ij} and σ_{ij} are the LJ energy and length parameters, respectively. The intramolecular nonbonded interactions between two atoms separated by three bonds are reduced by a factor of two.[51] The LJ parameters between different types of atoms (carbohydrate-water and carbohydrate-carbohydrate) were calculated using the Lorentz–Berthelot mixing rules,

$$\sigma_{ij} = \tfrac{1}{2}(\sigma_i + \sigma_j), \tag{5}$$

$$\varepsilon_{ij} = \sqrt{\varepsilon_i \varepsilon_j}. \tag{6}$$

The system of interest consisted of a single carbohydrate molecule (glucose, trehalose, or sucrose) in the presence of 300 water molecules in a cubic box. Therefore, no carbohydrate-carbohydrate interactions were present. The initial atomic coordinates of all three carbohydrate molecules were taken as their crystalline structures.[52–54] Periodic boundary conditions were applied to eliminate edge effects. Long-range electrostatic interactions were evaluated using the smooth particle mesh Ewald (SPME) method.[55,56] Specifically, 16 mesh lines in each dimension were chosen to provide a grid spacing around 1.2 Å, and a fourth-order B-spline interpolation was used. The Ewald convergence parameter α was set to 0.35 Å^{-1}. The cutoffs are described by two parameters: the point where the switching function begins (r_{c1}) and the point where it terminates (r_{c2}). A switching function was used to smoothly reduce the LJ and Coulombic interactions to zero between r_{c1}=8.0 Å and r_{c2}=9.5 Å. A long-range correction was also applied to the energy and virial calculations to account for the truncated long-range interactions.

To obtain the dynamical and structural properties of the water-carbohydrate solution, molecular dynamics simulations were performed in the *NVT* ensemble using a multiple time-step reversible reference system propagator algorithm (rRESPA).[57] In this rRESPA method, the forces associated with each atom are decomposed into three parts: short, medium, and long range. The short-range forces include contributions from bond stretching and bending, which have the shortest time scales. The medium-range forces contain the contributions from torsion, LJ, and direct-space Coulombic interactions within the cutoff. The long-range forces contain reciprocal-space Coulombic contributions that vary most slowly. The long-range forces were updated every 1 fs, while the short- and medium-range forces were updated every 0.25 and 0.5 fs, respectively. The temperature was controlled using five Nosé–Hoover thermostats.[58,59] In all of the *NVT* molecular dynamics (MD) simulations, the systems were equilibrated for at least 300 ps, followed by a production period of 1.5 ns. During the production run, configurations were saved every 50 fs.

To determine the densities of carbohydrate-water systems for *NVT* MD simulations, hybrid *NPT* Monte Carlo simulations were performed with a rRESPA algorithm.[60–62] In this method, multiple time-step MD moves in which atoms are moved simultaneously and deterministically are performed. The partition of interparticle interactions in the multiple time-step scheme was done identically to the one described above. The time step of each MD move was adjusted during the run to achieve an average Monte Carlo (MC) acceptance rate of 70%. In addition, the volume move and the hybrid displacement move (five MD steps) were set to be equally probable for every MC step. The *NPT* MC simulations were performed at temperatures of 0 and 30 °C

and at a pressure of 1 bar. Each *NPT* MC simulation was equilibrated for at least 300 000 MC steps. The density at each state point was determined by averaging the densities obtained during a production period of 500 000 MC steps.

In addition to the carbohydrate-water simulations, pure water simulations consisting of 300 water molecules were carried out in the same fashion under identical simulation conditions to provide reference bulk values of pure water properties for comparison. For instance, the density of water for *NVT* MD simulations was determined to be 0.999 and 0.996 through *NPT* MC simulations at 0 and 30 °C, respectively, under a pressure of 1 bar. The resulting density of pure water was found to be very similar to that of bulk water in carbohydrate-water solutions at both 0 and 30 °C; they differ by less than 5%. The density of bulk water in carbohydrate-water solutions was determined by first defining a 2-Å thick shell around the carbohydrate. The inner radius of the shell was set to be 8 Å from the center of mass of the carbohydrate molecule. The bulk water density was then calculated as the total number of water molecules in this shell divided by the volume of the shell.

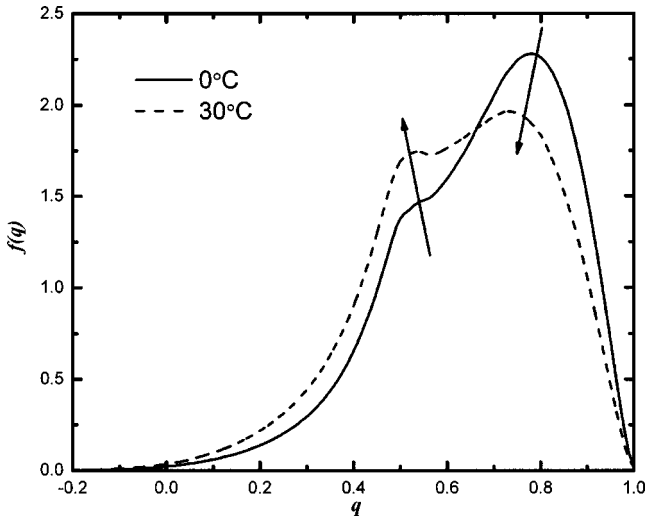

FIG. 2. The effect of temperature on the distribution of the orientational order q for pure water at $\rho=0.999$ (0 °C) and 0.996 g/cm^3 (30 °C). The fraction of molecules with q values between $q+dq/2$ and $q-dq/2$ is $f(q)dq$. The area under each curve is normalized to unity. Arrows show the trends with increasing temperature.

III. RESULTS AND DISCUSSION

A. Structure

We begin by showing the effects of carbohydrates on the structural order of proximal water molecules. The orientational order parameter q (Refs. 46 and 47) was employed to quantify the tendency of a water molecule and its four nearest neighbors to adopt a tetrahedral arrangement. The orientational order metric for water molecule i is given in

$$q_i = 1 - \frac{3}{8}\sum_{j>k}\left(\cos\psi_{ijk} + \tfrac{1}{3}\right)^2, \tag{7}$$

where ψ_{ijk} is the angle formed between the central oxygen atom i and its neighboring oxygen atoms j and k. This summation is over the six possible O–O–O angles involving the central molecule i and pairs of its four nearest neighbors. In our case, for water molecules near the carbohydrate, the four nearest neighbors can be either water or carbohydrate oxygen atoms. For a perfect tetrahedral arrangement, q is equal to 1 since the value of $\cos\psi_{ijk}$ is equal to $-1/3$. On the other hand, when the relative arrangement of the central atom and its neighbors is uncorrelated, the mean value of q vanishes, which corresponds to the ideal gas limit. As shown by Errington and Debenedetti,[47] the q distribution shows a bimodal character for pure water, suggesting that the statistics of the time-dependent spatial arrangement adopted by a water molecule with its four nearest neighbors are distributed around structured (ice-like, high-q peak) and unstructured (low-q peak) configurations.[63,64] Figure 2 shows this bimodal distribution at 0 and 30 °C for pure water with corresponding densities of 0.999 and 0.996 g/cm^3, respectively. The low-q peak is located approximately at 0.5 at both 0 and 30 °C, while the high-q peak is located around 0.78 at 0 °C and 0.74 at 30 °C.

To study the degree of water tetrahedrality in the vicinity of carbohydrate molecules, we calculated the q distribution of water molecules at various distances from the closest carbohydrate atoms (oxygen and carbon). In Fig. 3, the q distributions are shown for different water layers around the trehalose molecule at 0 °C. For water molecules that are far from the trehalose (9–10 Å), the q distribution is very similar to that for pure water. The tetrahedrality distribution for water molecules within less than 5 Å from the closest carbohydrate atom exhibits an appreciable decrease in the high-q peak with a corresponding increase in the low-q peak and in the low-q values ($0.1<q<0.4$). A similar trend is also observed for glucose and sucrose (not shown). This result clearly indicates that these three carbohydrates impose a destructuring effect on the surrounding water, which mimics the effect of a temperature increase as indicated in Fig. 2.

The tetrahedrality metric q was also computed for each water molecule and averaged over successive 0.5-Å shells as a function of distance from a specific carbohydrate atom,

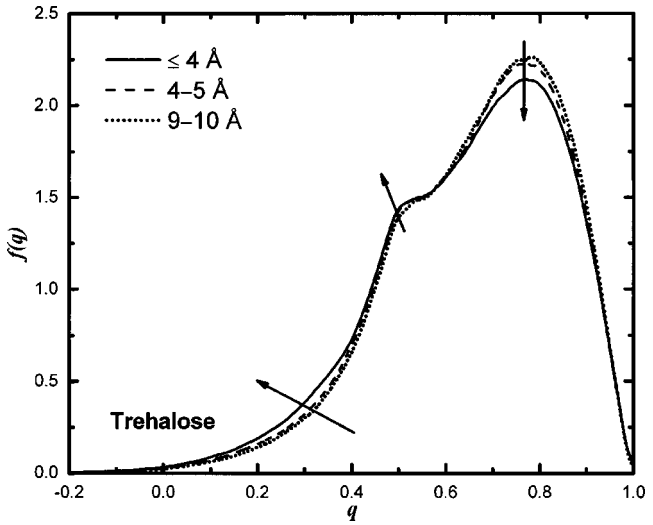

FIG. 3. The q distributions for trehalose at 0 °C. They were evaluated for water molecules that are less than 4 Å, between 4 and 5 Å, and between 9 and 10 Å, from the closest carbohydrate atoms (oxygen and carbon).

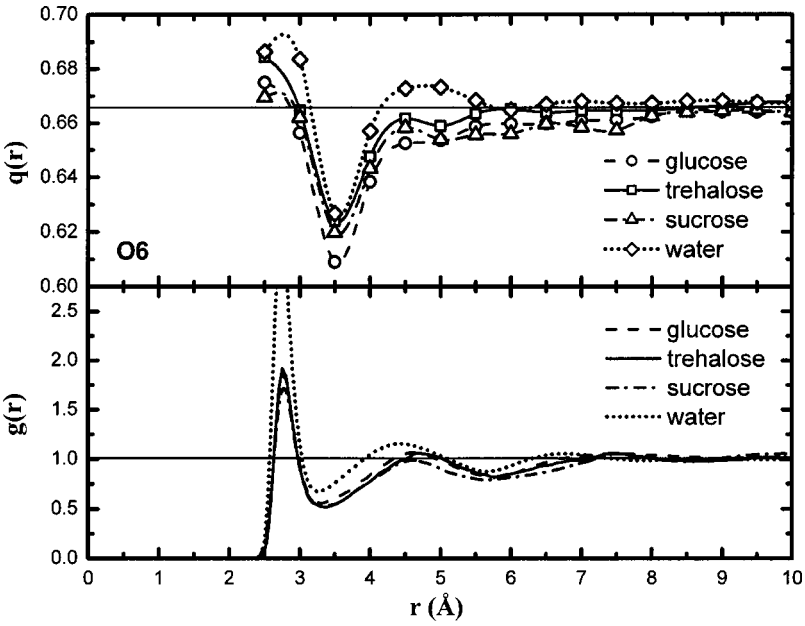

FIG. 4. Radial distributions of orientational order parameter $q(r)$ around carbohydrate hydroxyl oxygens (O6) as a function of carbohydrate type at 0 °C with the corresponding oxygen (carbohydrate)–oxygen (water) radial distribution functions $g(r)$. The $g(r)$ and $q(r)$ for pure water under the same simulation conditions are inserted in these figures for comparison. It should be noted that the $g(r)$ and $q(r)$ for water in the dilute carbohydrate-water solution are identical to those for pure water.

which gives a radial distribution of orientational order $q(r)$. This $q(r)$ radial distribution gives the average value of q for the water molecules in a specific hydration layer around a selected carbohydrate oxygen. Since the oxygen–oxygen radial distribution functions $g(r)$ of water oxygens around hydroxyl oxygens, such as O2 or O6 (Fig. 1), are similar to the oxygen–oxygen $g(r)$ of pure water, it is particularly interesting to compare the $q(r)$ of pure water to that of water molecules around these hydroxyl groups. Selected radial distributions of the orientational order parameter $q(r)$ around carbohydrate oxygens at 0 °C are shown in Figs. 4 and 5. In general, the hydroxyl oxygens that are not directly bonded to the carbohydrate ring (O6 of all three sugars, O6′ of trehalose and sucrose, and O2′ of sucrose) exhibit a trend similar to that found in pure water. Figure 4 depicts a typical $q(r)$ of water around these hydroxyl oxygens. The key feature to note is the lower average value of q for water molecules in the first and second hydration shell around O6 oxygens in comparison to the $q(r)$ for pure water. For the hydroxyl oxygens bonded directly to the carbohydrate ring, such as the O2 atoms of all three carbohydrates, the average values of q within 3.5 Å are comparably lower than those around O6 oxygens and fall below the bulk value for all three carbohydrates, as shown in Fig. 5. For water molecules around ring and glycosidic oxygens, the $q(r)$ reveals a considerably less structured solution environment (data not shown), the q values within 4 Å (0.2–0.50) falling entirely inside the range in Fig. 2 where water is characterized as "unstructured." We also observe a similar deviation of the tetrahedrality of water molecules around these carbohydrate atoms from that of bulk water at 30 °C (data not shown). The important conclusion from these calculations is that as water molecules approach the carbohydrate molecule, their local environment becomes

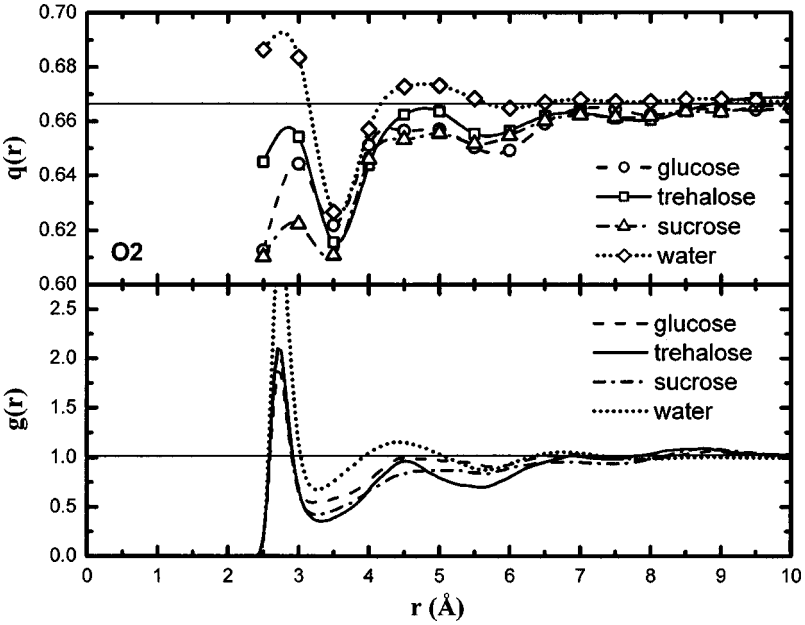

FIG. 5. Radial distributions of orientational order parameter $q(r)$ around carbohydrate hydroxyl oxygens (O2) as a function of carbohydrate type at 0 °C with the corresponding oxygen (carbohydrate)–oxygen (water) radial distribution functions $g(r)$. The $g(r)$ and $q(r)$ for pure water under the same simulation conditions are inserted in these figures for comparison. It should be noted that the $g(r)$ and $q(r)$ for water in the dilute carbohydrate-water solution are identical to those for pure water.

progressively less tetrahedral. An obvious cause of this is the steric constraint imposed by the carbohydrate molecule.

B. Translational and rotational dynamics

To examine water dynamics around the carbohydrate, it is necessary to treat both translational and rotational mobility as a local property. A local diffusion coefficient of water $D_{t\text{-local}}$ at a given distance r from a specific carbohydrate atom was calculated according to the following finite difference expression based on the Einstein relation:[65]

$$D_{t\text{-local}} = \frac{1}{6(t_2 - t_1)} (\langle |\boldsymbol{r}(t_2) - \boldsymbol{r}(0)|^2 - |\boldsymbol{r}(t_1) - \boldsymbol{r}(0)|^2 \rangle), \quad (8)$$

where $\boldsymbol{r}(t)$ is the position vector of a water molecule at time t. The values of t_1 and t_2 are set to 1 and 2 ps, respectively, based on the assumption that the diffusional regime can be reached after 1 ps and that water molecules, on the average, do not diffuse further than 2–3 Å from their initial location in 1 ps. We have verified that these two criteria are satisfied at both temperatures. The mean-square displacement was evaluated for each water molecule according to Eq. (8) and then averaged over water molecules located at a specified distance from the closest carbohydrate atom. The calculation was also preformed for selected sites on the carbohydrate ring in increments of 0.5 Å. Water molecules were assigned to a specific hydration shell depending upon their initial distance from the selected carbohydrate atom.

The rotational dynamics of water was analyzed by the autocorrelation function $\Gamma_2(t)$ given in

$$\Gamma_2(t) = \langle P_2(\boldsymbol{\mu}(0)\boldsymbol{\mu}(t)) \rangle, \quad (9)$$

where P_2 is the second-order Legendre polynomial and $\boldsymbol{\mu}(t)$ is the unit vector directed along the bisector of the H–O–H angle corresponding to the direction of the water dipole moment at time t. Similar to the evaluation of local diffusion coefficients, water molecules were assigned to a particular layer based on their initial position. Equation (9) was calculated for each water molecule for 2 ps and averaged over water molecules located at a specified distance from a given carbohydrate atom. To obtain the rotational correlation time $\tau_{c\text{-local}}$ from $\Gamma_2(t)$, Eq. (9) was first fitted to the stretched exponential or Kohlrausch–Williams–Watts function (KWW)[66,67] with two adjustable fitting parameters, $\beta (0 \leqslant \beta \leqslant 1)$ and τ, since it cannot be accurately described by a single exponential function. Given the values of β and τ extracted from a best fit, $\tau_{c\text{-local}}$ was then calculated by integrating the stretched exponential function from zero to infinity. Thus, the water diffusion coefficient and rotational correlation time were obtained as a function of the distance from specific carbohydrate atoms.

Figures 6 and 7 show the average diffusion coefficient and rotational correlation time of water molecules as a function of the distance from their closest carbohydrate atoms (carbon or oxygen) at 0 and 30 °C. For all three carbohydrates, both the translational and rotational motions of water are retarded in the vicinity of the carbohydrate molecule. In particular, the decrease in the translational and rotational mobility from the bulk values generally occurs in a region

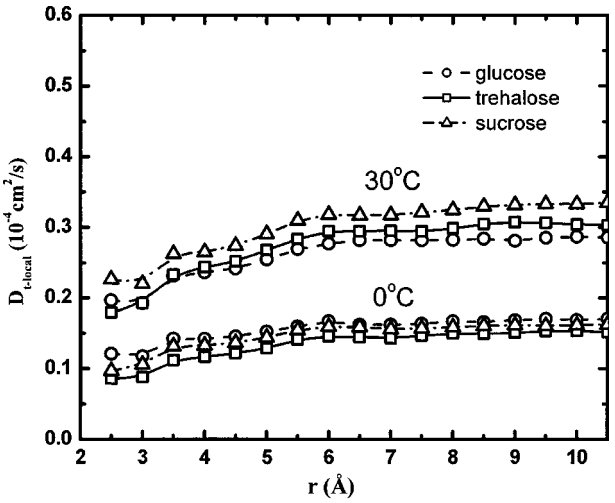

FIG. 6. Average translational diffusion coefficient of water around the carbohydrate (glucose, trehalose, and sucrose) as a function of initial distance to the closest carbohydrate atom (carbon and oxygen) at 0 and 30 °C.

within about 5.5 Å from the closest carbohydrate atoms. The bulk values for the water diffusion coefficient for the three carbohydrates examined here are slightly different from each other at both 0 and 30 °C. These small discrepancies are mainly due to the finite-size effects in our simulations. Despite these slight differences, the bulk values compare reasonably well with the water diffusion coefficients obtained in the pure water simulations at the density of 0.999 g/cm^3 (0 °C) and 0.996 g/cm^3 (30 °C), which are 0.16 and 0.30 $\times 10^{-4}$ cm^2/s, respectively. In addition, the rotational correlation time for pure water at these two densities (7.6 and 2.0 ps at 0.999 and 0.996 g/cm^3, respectively) agree with the bulk values in carbohydrate-water systems.

Figure 8 shows the local water diffusivities and rotational correlation times normalized by the corresponding bulk values. The most remarkable feature is the different temperature dependence of the translational and rotational motions of water molecules near the carbohydrate. For each carbohydrate, the water translational diffusion coefficients

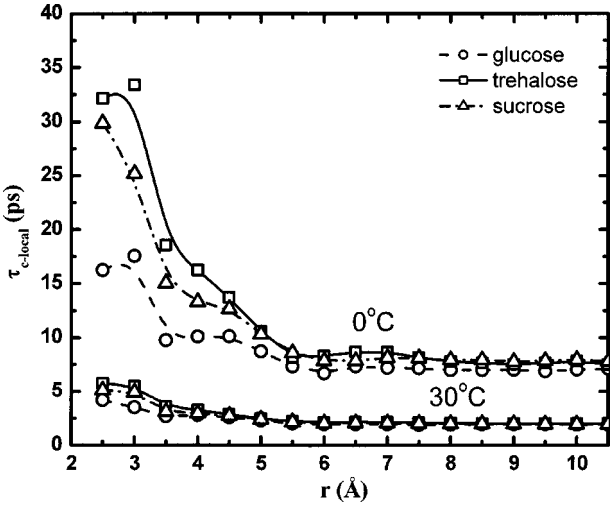

FIG. 7. Average rotational correlation time of water around the carbohydrate (glucose, trehalose, and sucrose) as a function of initial distance to the closest carbohydrate atom (carbon and oxygen) at 0 and 30 °C.

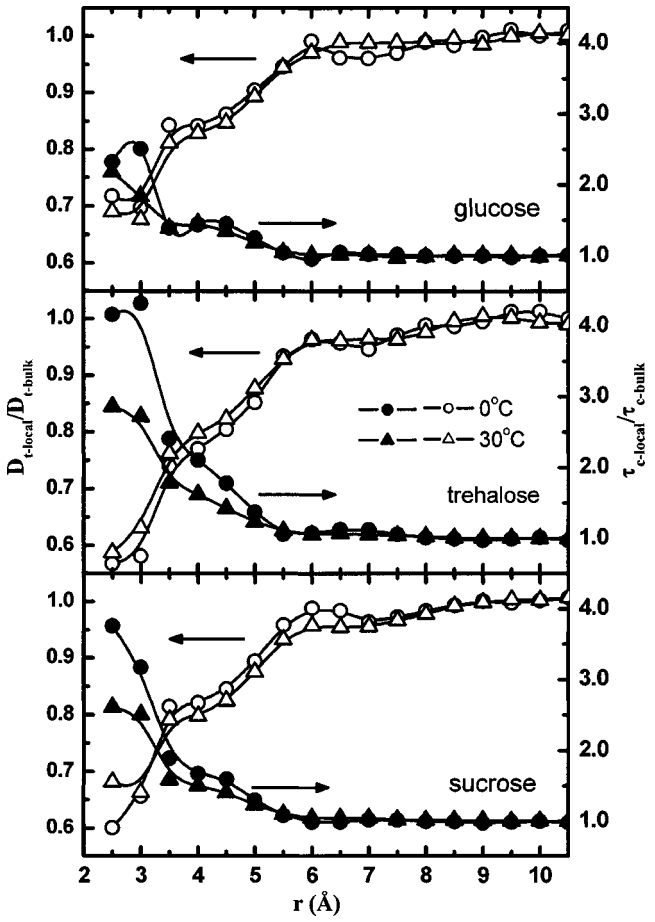

FIG. 8. Comparison of temperature effects on water translational diffusion coefficient and rotational correlation time as a function of initial distance to the closest carbohydrate atom for hydration water around glucose, trehalose, and sucrose. Quantities are normalized by the corresponding bulk values.

within the first and second hydration shells decrease by an approximately equal fraction of the bulk value at both temperatures. On the other hand, the decrease in water rotational mobility within the first and second hydration layers shows a considerable temperature dependence over the 0 to 30 °C range for the disaccharide molecules. The average rotational correlation time of water in the proximity of trehalose changes from roughly four times the bulk value at 0 °C to three times the bulk value at 30 °C. The different temperature dependence of the translational and rotational motions for these hydration water molecules is closely reminiscent of that for supercooled liquids.[68] At both 0 and 30 °C, the two disaccharides studied in this work retard the translational and rotational motions of the surrounding water molecules to a greater extent than does the monosaccharide, glucose. An explanation of this difference will be presented below.

To investigate the influence of different chemical groups along the carbohydrate ring on the mobility of the surrounding water, the translational diffusion coefficient and rotational correlation time were also evaluated for water molecules around different sites. For all three carbohydrates, although the values of $D_{t\text{-local}}$ and $\tau_{c\text{-local}}$ vary among different sites, no consistent conclusion can be drawn for the influence of different atom types on water dynamics. This is a consequence of the fact that these carbohydrates have both

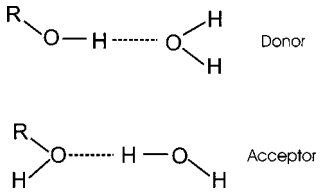

FIG. 9. Schematic representation of acceptor and donor carbohydrate-water H bonds.

polar and apolar groups in close proximity, which suggests that water dynamics are simultaneously influenced by different types of carbohydrate atoms. This result is consistent with the previous finding by Wang *et al.*[44] In their work, the calculation of the diffusion coefficient of water around the different atom types in maltose also shows that no general trend can be found.

C. Hydrogen bond analysis

The structure and dynamics of hydration water can be understood by analyzing the carbohydrate-water H-bond network and comparing it to that of bulk water. A geometric H bond definition[69] was used in this work. A hydrogen bond exists between two molecules if the oxygen–oxygen distance is less than 3.4 Å, while the O–H···O angle is greater than 120°. Our general conclusions do not change if the geometric criteria are varied by a small amount (e.g., ±0.2 Å and/or +20°). The carbohydrate-water H bonds were further classified as either acceptor or donor H bonds as defined in Fig. 9. Table I shows the average number of total carbohydrate-water H bonds per carbohydrate molecule $\langle N_{\text{HB-cw}}\rangle$, acceptor carbohydrate-water H bonds per carbohydrate molecule $\langle N_{\text{aHB-cw}}\rangle$, donor carbohydrate-water H bonds per carbohydrate molecule $\langle N_{\text{dHB-cw}}\rangle$, and water-water H bonds per water molecule $\langle N_{\text{HB-ww}}\rangle$ in the three carbohydrate-water systems at 0 and 30 °C. The results in Table I show no appreciable difference in $\langle N_{\text{HB-cw}}\rangle$ among the two disaccharides. The values of $\langle N_{\text{HB-cw}}\rangle$ compare well with published computational and experimental results for dilute carbohydrate solutions.[34,36] Conrad and de Pablo and Ekdawi-Sever calculated a $\langle N_{\text{HB-cw}}\rangle$ (hydration number) value of 13.4 for trehalose at 300 K and a value of 11.7 for sucrose at 353 K. These calculations were carried out at the 6 wt % carbohydrate concentration (1 carbohydrate molecule and 300 water molecules). Hydration numbers for glucose, sucrose, and trehalose at infinite dilution (298 °C) were also determined to be 8.4, 13.9, and 15.3, respectively, from ultrasound

TABLE I. Average number of total carbohydrate-water H bonds per carbohydrate molecule $\langle N_{\text{HB-cw}}\rangle$, carbohydrate-water acceptor H bonds per carbohydrate molecule $\langle N_{\text{aHB-cw}}\rangle$, carbohydrate-water donor H bonds per carbohydrate molecule $\langle N_{\text{dHB-cw}}\rangle$, and water-water H bonds per water molecule $\langle N_{\text{HB-ww}}\rangle$.

Type of H bond	T=0 °C	T=30 °C
glucose-water $\langle N_{\text{HB-wc}}\rangle$, $\langle N_{\text{aHB-wc}}\rangle$, $\langle N_{\text{dHB-wc}}\rangle$	9.3, 5.3, 4.0	8.8, 5.1, 3.7
trehalose-water $\langle N_{\text{HB-wc}}\rangle$, $\langle N_{\text{aHB-wc}}\rangle$, $\langle N_{\text{dHB-wc}}\rangle$	14.5, 8.4, 6.1	13.5, 7.9, 5.6
sucrose-water $\langle N_{\text{HB-wc}}\rangle$, $\langle N_{\text{aHB-wc}}\rangle$, $\langle N_{\text{dHB-wc}}\rangle$	14.6, 8.4, 6.2	13.3, 7.7, 5.6
water-water $\langle N_{\text{HB-ww}}\rangle$	3.2	3.0

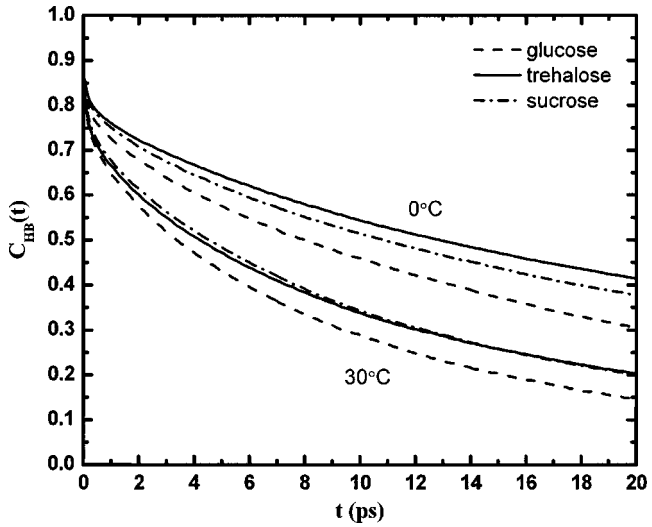

FIG. 10. Carbohydrate-water H-bond autocorrelation functions as a function of carbohydrate type at 0 and 30 °C.

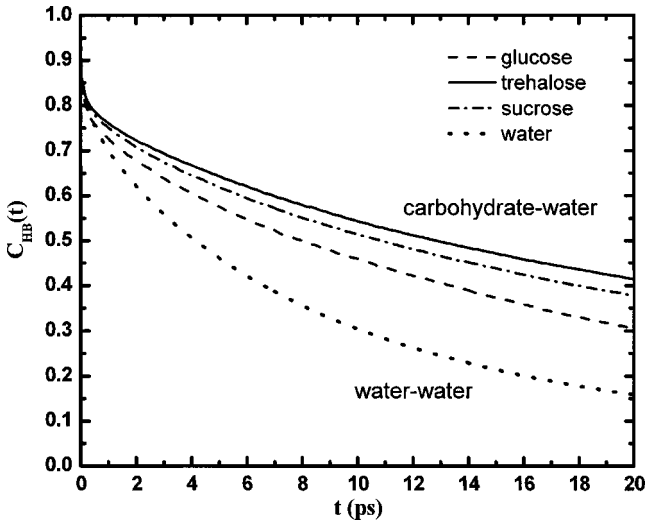

FIG. 11. Comparison of carbohydrate-water and water-water H-bond autocorrelation functions for different carbohydrates at 30 °C. It should be noted that the water-water H-bond autocorrelation functions calculated for pure water and for bulk water in glucose-water, trehalose-water, and sucrose-water simulations are identical.

measurements.[70] All three carbohydrates form slightly more acceptor H bonds with water at both temperatures. From the energetic point of view, the formation of donor H bonds is more favorable. The partial charge on a water oxygen atom ($-0.82\ e$) is more negative than those on carbohydrate oxygen atoms. These can be either $-0.683\ e$ (e.g., O6 in Fig. 1) or $-0.7\ e$ (e.g., O3 and O4 in Fig. 1), while the partial charge on the hydrogen atoms in water ($+0.40\ e$) and the hydroxyl groups of the carbohydrates ($+0.418\ e$ or $+0.435\ e$) are similar. However, the result in Table I suggests that entropic effects play a significant role in all three carbohydrate-water systems. One such entropic contribution arises from the fact that an acceptor bond can be formed in two equivalent ways (two H atoms per water molecule), whereas there is only one choice of H atom in a donor bond (see Fig. 9).

To characterize the carbohydrate-water and water-water H-bond dynamics, we calculated the H-bond autocorrelation function given in

$$C_{\mathrm{HB}}(t) = \frac{\langle h(0)h(t)\rangle}{\langle h\rangle}, \tag{10}$$

where $h(t)$ is a H-bond operator that takes the value of 1 when a tagged pair of oxygen atoms that belong to different molecules is H bonded, and 0 otherwise.[71] The bracket represents an average over all possible pairs of oxygen atoms and different time origins. $0.5N(N-1)\langle h\rangle$ gives the mean total number of carbohydrate-water or water-water H bonds in the system. This autocorrelation function $C_{\mathrm{HB}}(t)$ gives the probability that a H bond which exists $t=0$ remains intact at time t, independent of possible H-bond breaking at any intermediate time. Figure 10 shows the temporal behavior of carbohydrate-water $C_{\mathrm{HB}}(t)$ for glucose, trehalose, and sucrose at 0 and 30 °C. It can be seen that the H-bond autocorrelation function of glucose decays faster than those of the disaccharides at both 0 and 30 °C. It is also useful to examine the stability of carbohydrate-water H bonds relative to water-water H bonds. Figure 11 indicates that the H bonds formed between carbohydrate and water molecules are more resistant to the rearrangement in comparison to the water-water H bonds at 30 °C. A similar trend was found at 0 °C. This observation is significant in understanding why water dynamics are slowed down appreciably near the carbohydrate molecule, as discussed below.

The microscopic picture that emerges from the analysis of hydration water orientational order, water translational mobility, rotational correlation time, and H-bond dynamics is the following. In all three dilute carbohydrate solutions, the slow dynamics of hydration water molecules is primarily due to the formation of carbohydrate-water H bonds that are more stable than water-water H bonds, as evidenced by the decay in $C_{\mathrm{HB}}(r)$ (Fig. 11). This causes the translational and rotational motions of vicinal water molecules to be appreciably retarded (Figs. 6 and 7). Since liquid water is a connected random network of H bonds significantly exceeding the percolation threshold,[72,73] this slowing down effect cascades beyond the first hydration shell and eventually vanishes (>5 Å) when water-water H bonds begin to dominate (Figs. 6 and 7). Because the glucose molecule forms comparably less stable H bonds with the surrounding water molecules (Fig. 10), the decline in water translational and rotational motions near the glucose is less pronounced than those near the trehalose and sucrose (Fig. 8). Although carbohydrate and water molecules engage in appreciable H-bond formation, water near the carbohydrate molecule is unstructured in its tetrahedral arrangement with neighbors relative to the bulk. This is simply due to the steric constraint imposed by a stiff carbohydrate molecule, which reduces the free volume for the surrounding water molecules to occupy and adopt a perfect tetrahedral arrangement with their nearest neighbors. This steric hindrance is reflected in the diminished intensity of the first peak in the water-carbohydrate oxygen–oxygen $g(r)$, which is considerably lower than that in the oxygen–oxygen $g(r)$ of pure water (Figs. 4 and 5).

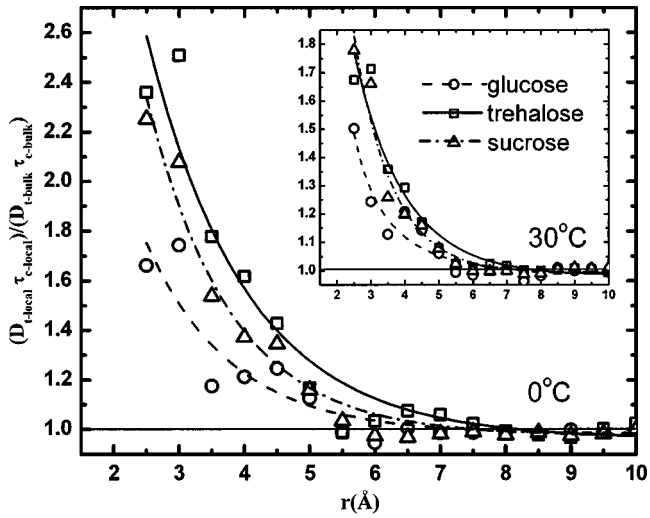

FIG. 12. Product of average translational diffusion coefficient and rotational correlation time of water molecules around the three carbohydrates, normalized by the corresponding bulk values, as a function of distance to the closest carbohydrate atom (carbon and oxygen) at 0 and 30 °C.

D. Decoupling of translational and rotational motions

To gain further insight on hydration water dynamics, we computed the product of water translational diffusion coefficient and rotational correlation time, normalized by their bulk values, as a function of distance from the closest carbohydrate atom (Fig. 12). According to the Stokes–Einstein (SE) and Debye–Stokes–Einstein (DSE) equations, this ratio is equal to

$$D_t\tau_c = \frac{kT}{6\pi\eta r_s}\frac{4\pi\eta r_s^3}{3kT} = \tfrac{2}{9}r_s^2, \tag{11}$$

where η is the viscosity and r_s is the hydrodynamic radius. The SE and DSE equations predict that the rotational and translational motions should have the same temperature and viscosity dependencies, and the product $D_t\tau_c$ should therefore be constant. Figure 11 shows the breakdown of this relationship for water molecules in the vicinity of a carbohydrate. This starts to occur at the edge of the secondary hydration shell (5 Å), where water translational and rotational motions begin to slow down. As the water molecules get closer to the carbohydrate molecule, their rotational dynamics starts to decrease at a faster rate than the corresponding translational mobility, meaning that water molecules translate further for every rotation they execute. As temperature decreases, the decoupling of water translational and rotational motions becomes more significant. The decoupling between translational and rotational dynamics is a canonical feature of deeply supercooled liquids.[19,24,74,75] The decoupling observed in this work, though enhanced at a lower temperature, is primarily a consequence of strong interactions between the carbohydrate and vicinal water molecules.

IV. SUMMARY

In the present work, we have sought to improve our fundamental understanding of the role of carbohydrates in pharmaceutical formulations through an extensive investigation of molecular-level carbohydrate-water interactions. Our calculations show a disruption of the tetrahedral arrangement of water molecules near the carbohydrate and a reduction in their translational and rotational mobility. The destructuring effect and slow dynamics are mainly due to the steric constraint imposed by a carbohydrate molecule on vicinal water molecules and its ability to form stable carbohydrate-water H bonds. Interestingly, hydration water translation and rotation show different temperature dependence and decouple from each other in the vicinity of the carbohydrate molecule. This decoupling is similar to that found in neat supercooled liquids.[19,24,74,75] When comparing the three sugars, no significant differences are found between trehalose and sucrose in their overall effects on the structural order q, translational diffusion coefficient $D_{t\text{-local}}$ and rotational correlation time $\tau_{c\text{-local}}$ of the surrounding water, but the disaccharides (trehalose and sucrose) restrict the translational and rotational dynamics of surrounding water molecules to a greater extent than glucose does.

The present study will be continued and extended to more concentrated carbohydrate-water systems at various temperatures, with the aim of covering a wider range of concentrations and temperatures, where translational and rotational motions of carbohydrate molecules decouple from those of water molecules.[17,19,24] The future work will focus on understanding the origin of decoupling phenomena reported in these previous studies.[17,19,24]

ACKNOWLEDGMENTS

We gratefully acknowledge the support of the Department of Energy, Division of Chemical Sciences, Geosciences, and Biosciences, Office of Basic Energy Science (Grant No. DE-FG02-87ER13714). We also thank C. J. Roberts and V. K. Shen for helpful discussions.

[1] L. M. Crowe, R. Mouradian, J. H. Crowe, S. Jackson, and C. Womersley, Biochim. Biophys. Acta **769**, 141 (1984).
[2] J. H. Crowe, S. B. Leslie, and L. M. Crowe, Cryobiology **31**, 355 (1994).
[3] C. Schebor, L. Burin, M. P. Buera, J. M. Aguilera, and J. Chirife, Biotechnol. Prog. **13**, 857 (1997).
[4] T. J. Anchordoguy, A. S. Rudolph, J. F. Carpenter, and J. H. Crowe, Cryobiology **24**, 324 (1987).
[5] T. Lin and S. N. Timasheff, Protein Sci. **5**, 372 (1996).
[6] A. Ramos, N. D. H. Raven, R. J. Sharp *et al.*, Appl. Environ. Microbiol. **63**, 4020 (1997).
[7] S. D. Allison, T. W. Randolph, M. C. Manning, K. Middleton, A. Davis, and J. F. Carpenter, Arch. Biochem. Biophys. **171**, 171 (1998).
[8] S. N. Timasheff, Annu. Rev. Biophys. Biomol. Struct. **22**, 67 (1993).
[9] J. F. Carpenter, K.-I. Izutsu, and T. W. Randolph, in *Freeze-Drying/Lyophilization of Pharmaceutical and Biological Products*, edited by L. Rey and J. C. May (Marcel Dekker, New York, 1999), Vol. 96, p. 123.
[10] J. F. Carpenter and J. H. Crowe, Cryobiology **25**, 244 (1988).
[11] F. Franks, Pure Appl. Chem. **65**, 2527 (1993).
[12] J. H. Crowe, J. F. Carpenter, and L. M. Crowe, Annu. Rev. Physiol. **60**, 73 (1998).
[13] E. Y. Shalaev and G. Zografi, J. Pharm. Sci. **85**, 1137 (1996).
[14] P. D. Orford, R. Parker, and S. G. Ring, Carbohydr. Res. **196**, 11 (1990).
[15] Y. Roos, Carbohydr. Res. **238**, 39 (1993).
[16] R. G. Strickley and B. D. Anderson, J. Pharm. Sci. **86**, 645 (1997).
[17] D. Girlich and H.-D. Lüdemann, Z. Naturforsch. C **49c**, 250 (1994).
[18] G. R. Moran and K. R. Jeffrey, J. Chem. Phys. **110**, 3472 (1999).
[19] M. Rampp, C. Buttersack, and H.-D. Lüdemann, Carbohydr. Res. **328**, 561 (2000).

[20]I. J. van den Dries, D. van Dusschoten, M. A. Hemminga, and E. van der Linder, J. Phys. Chem. B **104**, 10126 (2000).
[21]C. Branca, S. Magazù, G. Maisano, and P. Migliardo, J. Chem. Phys. **111**, 281 (1999).
[22]A. Faraone, S. Magazù, R. E. Lechner, S. Longeville, G. Maisano, D. Majolino, P. Migliardo, and U. Wanderlingh, J. Chem. Phys. **115**, 3281 (2001).
[23]S. Magazù, R. E. Lechner, S. Longeville, G. Maisano, D. Majolino, P. Migliardo, and U. Wanderlingh, Physica B **276**, 475 (2000).
[24]D. Champion, H. Hervet, G. Blond, M. L. Meste, and D. Simatos, J. Phys. Chem. B **101**, 10674 (1997).
[25]D. Girlich and H.-D. Lüdemann, Z. Naturforsch. C **49c**, 258 (1994).
[26]M. Feeney, C. Brown, A. Tsai, D. Neumann, and P. G. Debenedetti, J. Phys. Chem. B **105**, 7799 (2001).
[27]S. Magazù, G. Maisano, D. Majolino, P. Migliardo, A. M. Musolino, and V. Villari, Prog. Theor. Phys. Suppl. **126**, 195 (1997).
[28]C. Branca, S. Magazù, G. Maisano, P. Migliardo, and G. Romeo, J. Phys. Chem. B **105**, 10140 (2001).
[29]C. Branca, S. Magazù, G. Maisano, S. M. Bennington, and B. Fåk, J. Phys. Chem. B **107**, 1444 (2003).
[30]Q. Liu, R. K. Schmidt, B. Teo, P. A. Karplus, and J. W. Brady, J. Am. Chem. Soc. **119**, 7851 (1997).
[31]S. Engelsen and S. Pérez, J. Phys. Chem. B **104**, 9301 (2000).
[32]M. C. Donnamaria, E. I. Howard, and J. R. Grigera, J. Chem. Soc., Faraday Trans. **90**, 2731 (1994).
[33]G. Bonanno, R. Noto, and S. L. Fornili, J. Chem. Soc., Faraday Trans. **94**, 2755 (1998).
[34]P. B. Conrad and J. J. de Pablo, J. Phys. Chem. A **1999**, 4049 (1999).
[35]S. Engelsen and S. Pérez, Carbohydr. Res. **292**, 21 (1996).
[36]N. C. Ekdawi-Sever, P. B. Conrad, and J. J. de Pablo, J. Phys. Chem. A **105**, 734 (2000).
[37]E. R. Caffarena and J. R. Grigera, Carbohydr. Res. **300**, 51 (1997).
[38]E. R. Caffarena and J. R. Grigera, Carbohydr. Res. **315**, 63 (1999).
[39]C. J. Roberts and P. G. Debenedetti, J. Phys. Chem. B **103**, 7308 (1999).
[40]S. Engelsen, C. Monteiro, C. de Penhoat, and S. Pérez, Biophys. J. **93**, 103 (2001).
[41]C. Andersson and S. Engelsen, J. Mol. Graphics Modell. **17**, 101 (1999).
[42]J. Behler, D. W. Price, and M. G. B. Drew, Phys. Chem. Chem. Phys. **3**, 588 (2001).
[43]Q. Liu and J. W. Brady, J. Phys. Chem. B **101**, 1317 (1997).
[44]C. X. Wang, W. Z. Chen, V. Tran, and R. Douillard, Chem. Phys. Lett. **251**, 268 (1996).
[45]M. Sakurai, M. Murata, Y. Inoue, A. Hino, and S. Kobayashi, Bull. Chem. Soc. Jpn. **70**, 847 (1997).
[46]P.-L. Chau and A. J. Hardwick, Mol. Phys. **93**, 511 (1998).
[47]J. R. Errington and P. G. Debenedetti, Nature (London) **409**, 318 (2001).
[48]C. C. Liew, H. Inomata, and K. Arai, Fluid Phase Equilib. **144**, 287 (1998).
[49]K. Toukan and A. Rahman, Phys. Rev. B **31**, 2643 (1985).
[50]H. J. C. Berendsen, J. R. Grigera, and T. P. Straatsma, J. Phys. Chem. **91**, 6269 (1987).
[51]W. Damm, A. Frontera, J. Tirado-Rives, and W. L. Jorgensen, J. Comput. Chem. **18**, 1955 (1997).
[52]G. M. Brown, D. C. Rohrer, B. Berking, C. A. Beevers, R. O. Gould, and R. Simpson, Acta Crystallogr., Sect. B: Struct. Crystallogr. Cryst. Chem. **B28**, 3145 (1972).
[53]G. M. Brown and H. A. Levy, Acta Crystallogr., Sect. B: Struct. Crystallogr. Cryst. Chem. **B29**, 790 (1972).
[54]S. S. C. Chu and G. A. Jeffrey, Acta Crystallogr., Sect. B: Struct. Crystallogr. Cryst. Chem. **B24**, 830 (1968).
[55]T. Darden, D. M. York, and L. G. Pedersen, J. Chem. Phys. **98**, 10089 (1993).
[56]U. Essmann, L. Perera, M. L. Berkowitz, T. Darden, H. Lee, and L. G. Pedersen, J. Chem. Phys. **103**, 8577 (1995).
[57]M. Tuckerman, B. J. Berne, and G. Martyna, J. Chem. Phys. **97**, 1990 (1992).
[58]G. J. Martyna, M. L. Klein, and M. Tuckerman, J. Chem. Phys. **97**, 2635 (1992).
[59]G. J. Martyna, M. Tuckerman, D. Tobias, and M. L. Klein, Mol. Phys. **87**, 1117 (1996).
[60]B. Mehlig, D. W. Heermann, and B. M. Forrest, Phys. Rev. B **45**, 679 (1992).
[61]J. J. de Pablo and D. Gromov, J. Chem. Phys. **103**, 8247 (1995).
[62]P. Attard, J. Chem. Phys. **116**, 9616 (2002).
[63]M.-C. Bellissent-Funel, Europhys. Lett. **42**, 161 (1998).
[64]A. K. Soper and M. A. Ricci, Phys. Rev. Lett. **84**, 2881 (2000).
[65]V. Lounnas, B. M. Pettitt, and G. N. Phillips, Biophys. J. **66**, 601 (1994).
[66]G. Williams and D. C. Watts, Trans. Faraday Soc. **66**, 80 (1970).
[67]R. Kohlrausch, Ann. Phys. **12**, 353 (1847).
[68]M. D. Ediger, Annu. Rev. Phys. Chem. **51**, 99 (2000).
[69]J. Tirado-Rives and W. L. Jorgensen, J. Am. Chem. Soc. **112**, 2773 (1990).
[70]S. A. Galema and H. Høiland, J. Phys. Chem. **95**, 5321 (1991).
[71]D. Chandler and A. Luzar, Nature (London) **379**, 55 (1996).
[72]A. Geiger, F. H. Stillinger, and A. Rahman, J. Chem. Phys. **70**, 4185 (1979).
[73]H. E. Stanley and J. Teixeira, J. Chem. Phys. **73**, 3404 (1980).
[74]C.-Y. Wang and M. D. Ediger, J. Phys. Chem. B **104**, 1724 (2000).
[75]M. T. Cicerone and M. D. Ediger, J. Chem. Phys. **104**, 7210 (1996).